Naturally occurring reverse tilt domains in a high-pretilt alignment nematic liquid crystal

Ruiting Wang, Timothy J. Atherton, Minhua Zhu,* Rolfe G. Petschek, and Charles Rosenblatt
Department of Physics, Case Western Reserve University, Cleveland, Ohio 44106-7079, USA
(Received 22 May 2007; published 9 August 2007)

A cell whose substrates were coated with the polyamic acid SE1211 (Nissan Chemical Industries) and baked at high temperatures was filled with a nematic liquid crystal in the isotropic phase. On cooling into the nematic phase, naturally occurring and temporally and thermally robust reverse tilt domains separated by thin filamentlike walls were observed. The properties of these structures are reported.

DOI: 10.1103/PhysRevE.76.021702 PACS number(s): 61.30.Jf

The broad category of reverse tilt domains (RTDs) refers to a spatially rapid variation of the liquid crystal director along a plane that, when viewed from above, is associated with a disclination line. Because RTDs tend to diminish the quality of a liquid crystal device, there has been considerable research into understanding and eliminating them. There are two common varieties of RTDs: One is associated with domain walls between positive and negative twists in a nematic liquid crystal [1,2], which can be eliminated by incorporating cholesteric additives. The second type, which is the variety most often associated with the term "reverse tilt domain," occurs in a planar cell when the liquid crystal is subjected to an applied electric or magnetic field above the Freedericksz transition threshold: In one region the director has a polar orientation $+\theta$, and in an adjacent region an orientation $-\theta$ [3,4]; a domain wall then separates the two regions. This type of RTD structure occurs most commonly in planar cells treated for a uniform azimuthal orientation by means of mechanical rubbing or irradiation of a polymer-coated substrate, and can be obviated by introducing a small uniform pretilt angle relative to the planar orientation. In this paper we report on textures due to RTDs that occur naturally in cells treated for a high pretilt angle θ_0, where we define θ_0 as the angle relative to the *vertical* direction; thus $\theta_0=0$ would correspond to homeotropic orientation. We find that the optical contrast between the domains and the filamentlike domain walls decreases with increasing temperature in the nematic phase, completely disappearing in the isotropic phase. However, on cooling back into the nematic phase, the textures reappear in the same locations, indicating a strong surface memory effect [5–7].

Two microscope glass slides were cleaned and spin coated with the polyamic acid SE1211 (Nissan Chemical Industries), then baked for 1 h at a temperature of 240° C. After baking, the imidized SE1211 has a relatively rigid backbone that promotes planar alignment, as well as alkyl side chains that promote homeotropic alignment [8–10]. Had we baked using the manufacturer's specifications of 180° C for 50 min, SE1211 would have induced vertical (homeotropic) alignment in the liquid crystal. Higher temperature baking, however, further imidizes the backbone and cleaves off a fraction of the side chains, resulting in a large, controllable, and robust pretilt angle θ_0 relative to the vertical direction; this is the case for the baking regimen used in our experiments. Without being rubbed, the two substrates were placed together, separated by mylar spacers, and cemented. The thickness of the empty cell was measured by interferometry and found to be $d=4.5\pm0.2$ μm. The cell then was filled with liquid crystal ZLI-4330, which is a negative dielectric anisotropy mixture manufactured by Merck, in the isotropic phase and then cooled through the clearing temperature $T_{NI}=82°$ C to room temperature in the nematic phase. A typical sample is shown in the polarized photomicrographs in Fig. 1. Although the studies described herein were performed on ZLI-4330, similar textures were observed with two other Merck liquid crystal mixtures, MLC-6610 and E7, the latter being a positive dielectric anisotropy mixture.

Figure 1 shows a superposition of two textures at four different temperatures. The Schlieren texture comes about because there is no imposed azimuthal easy axis over the entire field of view; rather, the local easy axis is due to the randomly oriented polymer and evaporation of the solvent. In addition, there is a superimposed texture of filamentlike domain walls, which will be discussed in the next paragraph. The Schlieren texture indicates that the azimuthal orientation φ of the director varies with position, and the dark brushes shift relative to the cell as the cell is rotated between crossed polarizers. This texture is analogous to what is observed in a cell with random planar alignment. Two items should be noted: defects with both two and four brushes can be observed, and the contrast between the dark Schlieren brushes and lighter background regions is highest when the polarizer and analyzer are mutually perpendicular, indicating the absence of a twist deformation with an axis along the normal to the substrates. This absence of twist might be surprising,

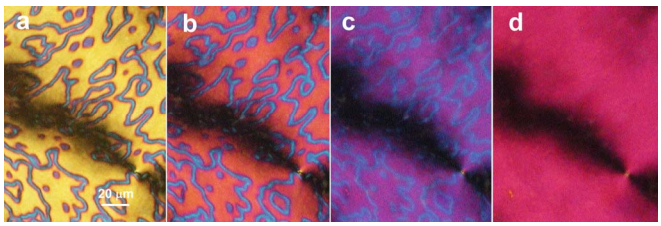

FIG. 1. (Color online) Polarized photomicrograph of textures, showing superposition of pinned filaments and Schlieren brushes. (a) $T=25°$ C, (b) $T=40°$, (c) $T=55°$, and (d) $T=70°$. Bar corresponds to 20 μm.

*Present address: Kent Optronics, Hopewell Junction, NY 12553, USA.

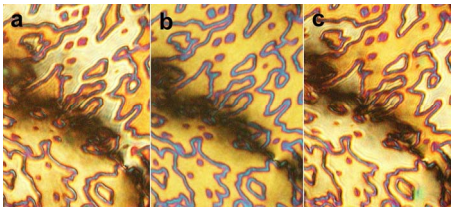

FIG. 2. (Color online) Polarized photomicrographs of textures illuminated with collimated white light at polar angles: (a) 0°, i.e., normal incidence, (b) at angle +20°, and (c) at −20° with respect to the substrate normal.

given the expectation that there has been no organized rubbing. We suppose, in consequence, that the preferred azimuthal direction is either random or controlled by some memory effect that is induced after the cell is assembled, e.g., by flow induced alignment when the cell is first filled. The observed Schlieren texture, however, clearly indicates random alignment, which is inconsistent with quasi-uniform flow alignment. Therefore we would expect there to be different alignment mechanisms at the two surfaces: Most likely one surface—this probably is the surface at which the nematic phase first nucleates—controls the alignment, with the effects of the other being relatively unimportant.

The filament texture is characterized by a variation in brightness and color across the width of the filament, which is symmetric about the filament's center. Located on either side of the filament are larger domains of approximately uniform color. On rotating the cell between crossed polarizers, the filaments and domains rotate together with the cell with virtually no change in appearance, except for becoming dark as the Schlieren brushes pass through. The continuity of the Schlieren brushes implies a continuity of the in-plane director component. However, when the cell is illuminated with a collimated white light source that is tilted by approximately 20° with respect to the substrate normal, the two formerly uniform domains on either side of a given filament no longer are identical in appearance (Fig. 2, with color online). These observations would suggest that although the projection of the director orientation in the plane of the cell is continuous across the filament, the polar orientation corresponds to $+\theta_0$ in one domain and $-\theta_0$ in the other. In consequence, the director may vary across the filament in several ways: (i) as a 180° azimuthal variation at a fixed (or varying) magnitude $|\theta_0|$, (ii) as a variation of $|\theta|$ through $\theta=0°$ (the vertical direction), or (iii) as a variation of $|\theta|$ through $\theta=90°$ (the planar direction). Mechanisms (i) and (ii) would require that at least one dark stripe appear throughout the length of the filament, independent of the filament's local orientation as it snakes through the cell; this does not occur. Thus, we conclude that $|\theta|$ varies across the filament, being approximately planar in the center of the filament; this would correspond to the classic RTD geometry. More evidence will be presented below.

Let us first consider the domain walls at room temperature, Fig. 1(a). The width of a filament (wall) between two RTDs reflects a compromise between the bulk elastic energy of the nematic and the surface anchoring energy, which favor a wider and narrower wall, respectively. A typical size L for the domain wall may be estimated by inserting a trial director configuration into the free energy and minimizing with respect to L. We adopt a coordinate system where z is perpendicular to the substrates, y lies along the length of the wall, and x across the wall's width. Assuming a single elastic constant K and a polar orientation θ that is independent of z, a simple but reasonable ansatz is

$$\theta(x) = \begin{cases} -\theta_0 & x < -L/2 \\ 2\theta_0 x/L & -L/2 \le x < L/2 \\ +\theta_0 & x \ge L/2 \end{cases},$$

where the director $\hat{n}=[\sin\theta, 0, \cos\theta]$. The energy F per unit length of the wall for this configuration may be calculated within the single elastic constant approximation and by using the Rapini-Papoular form [11] for the anchoring energy. By exploiting the symmetry about $x=0$, we find [12]

$$F = 2\left[\frac{1}{2}Kd\int_0^{L/2}(d\theta/dx)^2dx + \frac{1}{2}W_\theta\int_0^{L/2}\sin^2[\theta(x)-\theta_0]dx\right]$$

$$= 2d\frac{K\theta_0^2}{L} + \frac{LW_\theta}{4}(1-\operatorname{sinc} 2\theta_0), \quad (1)$$

where W_θ is the polar anchoring strength coefficient. F is minimized for $L=2\sqrt{2}\theta_0\sqrt{Kd/W_\theta}(1-\operatorname{sinc} 2\theta_0)^{-1/2}$. On inserting $\theta_0 \sim 30°$—we shall see later that this is a typical value near room temperature—$d=4.5$ μm, $K\sim 10^{-6}$ dyn [12], and a value for $W_\theta \sim 0.1$ erg cm^{-2} [10], we find the width of the domain wall $L\sim 2$ μm, which is in good agreement with the polarizing microscope images.

Turning now to the temperature variation of the textures, we observe that the contrast between the domains and filaments decreases when the cell is heated, nearly vanishing even before the liquid crystal enters the isotropic phase. After heating into the isotropic phase and cooling back into the nematic, the filament textures are observed to reappear in the same locations, independent of the length of time (up to at least 10 h) that the liquid crystal is held in the isotropic phase before recooling. This is indicative of a robust surface memory effect [5–7]. To understand the temperature variation of the textures, we prepared the substrates of an Abbe refractometer for vertical alignment and filled the gap with liquid crystal. We then measured the ordinary and extraordinary refractive indices, n_o and n_e respectively, of ZLI-4330; the refractive indices and the birefringence Δn are shown in Fig. 3. We then examined a cell whose surfaces were treated with SE1211 as described above, but also rubbed extremely weakly in order to provide a uniform azimuthal orientation for the director. The cell, along with a Babinet-Soleil compensator, was placed between crossed polarizers oriented at 45° with respect to the rubbing direction in the path of the beam from a He-Ne laser. A 100 μm diameter pinhole was placed over the cell to limit the size of the region sampled by the laser. The optical retardation α of the cell was measured as a function of temperature by adjusting the compensator to null the intensity at the downstream detector. Because the substrates were rubbed mutually antiparallel, the polar angle θ was uniform throughout the cell and equal to the pretilt angle θ_0. Thus θ_0 was extracted as a function of temperature

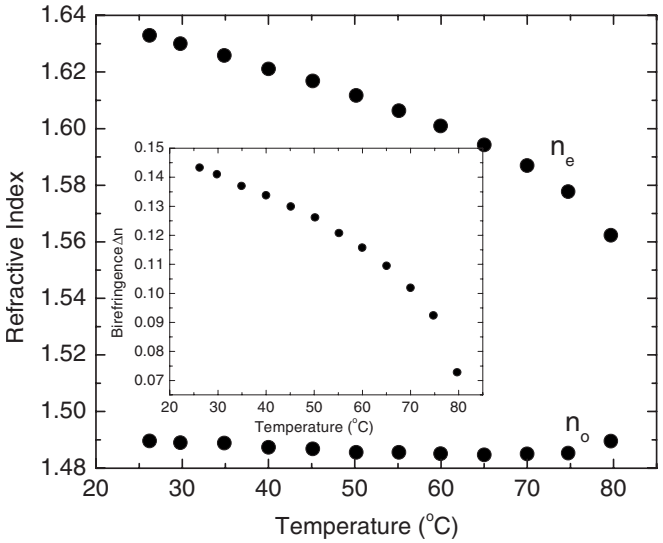

FIG. 3. Ordinary and extraordinary refractive indices n_o and n_e vs temperature for ZLI-4330 at wavelength $\lambda=633$ nm. Inset: Birefringence Δn.

from the equation $\alpha=2\pi d/\lambda\ [(\cos^2\theta_0/n_o^2+\sin^2\theta_0/n_e^2)^{-1/2}-n_o]$ and is shown in Fig. 4. It is clear that the pretilt angle θ_0 increases with increasing temperature at a substrate coated with SE1211, an effect that has been observed for other liquid crystals, although for smaller values of θ_0 [9]. For the present case it would suggest that the proposed director variation across the filament in regions where the azimuthal (in-plane) component of the director orientation $\hat{n}_\varphi$ is approximately perpendicular to the filament is comprised of a combination of splay and bend distortion, and in regions where $\hat{n}_\varphi$ is parallel to the filament it is comprised of twist distortion. (See cartoon in Fig. 5.) Nevertheless, for both cases the director approaches the planar orientation ($|\theta_0| \rightarrow 90°$) with elevated temperature in the domains on either side of the filament, resulting in a decrease of optical contrast across the filament (Fig. 1). This is consistent with the near disappearance of the filaments at high temperatures, but at temperatures that are still within the nematic phase. In fact,

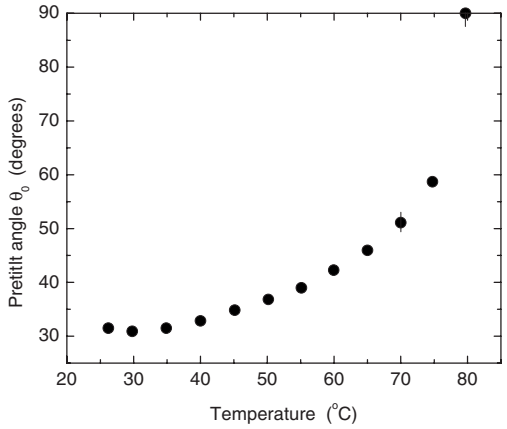

FIG. 4. Pretilt angle θ_0 vs temperature, where θ_0 is the angle with respect to the *vertical* direction.

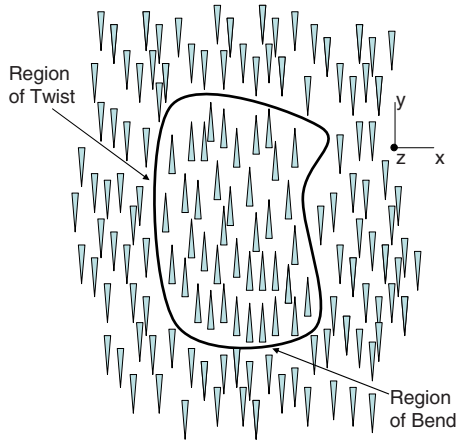

FIG. 5. (Color online) Schematic diagram of proposed director alignment in the domains around the filament (shown as false color black). The vertex of isosceles triangle represents the z component of the director pointing downward, and the base of triangle represents the z component pointing upward. Where the projection of the director in the xy plane is parallel to the filament, the director undergoes a twist deformation across the domain wall; where the projection of the director is perpendicular to the filament, the director undergoes a primarily bendlike deformation across the domain wall.

we believe that it is the large pretilt angle, i.e., nearly—but not quite—planar orientation, at high temperatures that is responsible for nature of the observed reverse tilt domains. On first cooling from the isotropic to the nematic phase, where the director is nearly planar, the energy cost of a nearly pure bend deformation or pure twist deformation associated with a relatively small polar angle variation $\Delta\theta=180°-2\theta_0$ of the director across the domain wall would be much smaller than that of a corresponding azimuthal variation $\Delta\varphi=180°$ of the director at constant θ. Although the pretilt angle θ_0 decreases as the temperature is reduced, thereby decreasing the energy advantage of the polar variation of the director, no obvious change in the character of the RTD is observed. There are two possible reasons for this. First, there may be sufficiently strong surface memory effects [5–7] so that throughout the experimental temperature range, RTDs with polar changes in the director are thermodynamically stable. If this were the case, we could use this information to estimate the memory effects on the anchoring strength in these cells. Unfortunately, however, azimuthal and polar variations through the RTD walls are topologically distinct, which is the second reason for the absence of qualitative changes in the RTDs and filaments with temperature. The topological distinctness can be seen by noting that $\hat{n} \rightarrow -\hat{n}$, and thus $\hat{n}_\varphi$ rotates by 180°, if we move along the following path in the xy plane: (i) traverse through a RTD wall through which the director undergoes a polar variation of $180°-2\theta_0$, (ii) move partially through an ordered domain, (iii) cross a RTD wall through which the director undergoes an azimuthal rotation of 180°, and (iv) return to the original location. This implies that there is a topological defect—a standard nematic disclination—enclosed within this path. We conclude that even if it were energetically favorable to change from a polar wall, which is expected to form when

$\theta_0 - 90°$ near the nematic-isotropic transition, to an azimuthal variation RTD wall, then actually making this change would require a nucleation step in which a disclination loop forms in the polar variation RTD. This loop would then need to grow and separate into two disclination lines that terminate at the surfaces. As there would be an azimuthal variation RTD wall between these two disclination lines, and if such walls have lower energies, this would result in a decrease in energy when these lines have separated sufficiently far apart. However, for small separations, the energy would *increase* by substantially more than the thermal energy. Therefore, we expect that azimuthal variation RTD walls will *not* form, whether or not they lower the energy.

We can understand the energetics more quantitatively by removing the restriction that θ is independent of z, as was used in deriving Eq. (1). That is, away from the surfaces the elastic distortion of the director may take place over a longer length scale in the xy plane, thus reducing the overall elastic energy. Consider the situation that n_φ is approximately perpendicular to the domain wall. There are two limiting cases: When the director is nearly homeotropic, an azimuthal rotation of the director through 180° corresponds to the minimum energy configuration. On the other hand, when the director is nearly planar, then a polar rotation from $\theta = -\theta_0$ to $\theta = +\theta_0$ is energetically most favorable. We quantified this behavior by examining two cases: (i) a wall where the director is constrained to a fixed value $\theta = \theta_0$ but is allowed to rotate azimuthally, and (ii) a wall for which the azimuthal orientation φ is fixed but θ is allowed to vary. These approximations clearly are valid only near the limiting cases described; at intermediate pretilts, the director field may include both azimuthal and polar distortions. In two dimensions and admitting separate values K_{11}, K_{22}, and K_{33} for the splay, twist, and bend elastic constants, respectively, the Euler-Lagrange equations for the director field that minimize the free energy are nonlinear and must be solved numerically. We formed an implicit finite-difference representation of the Euler-Lagrange equations over a rectangular grid and solved them iteratively by the Newton method; values for d and W_θ were those used above and values for the elastic constants were taken as $K_{11} = 10^{-6}$ dyn, $K_{33}/K_{11} = 1.46$ [13], and $K_{22}/K_{11} = 0.5$; W_φ/W_θ was set to a typical value of 0.1 [14,15], where W_φ is the azimuthal anchoring strength coefficient, which itself may depend on θ_0. The free energies per unit length of the polar and azimuthal configurations were calculated from the respective solutions, and are plotted as a function of pretilt angle in Fig. 6. The results show that for the large initial pretilt angles θ_0 that occur on cooling from the isotropic into the nematic phase, the polar-type RTD filament is energetically most favorable, and remains in place even on cooling to sufficiently low temperatures where θ_0 becomes small, i.e., approaching the homeotropic orientation. Although the crossover value of θ_0 obviously depends on the elastic and anchoring parameters, the calculation clearly demonstrates that the initial high pretilt at elevated temperatures results in the observed RTDs. These calculations also suggest that an azimuthal variation RTD wall may be the thermodynamically stable state at room temperature. However, as discussed above, the absence of observations of such RTD walls is likely controlled by kinetics.

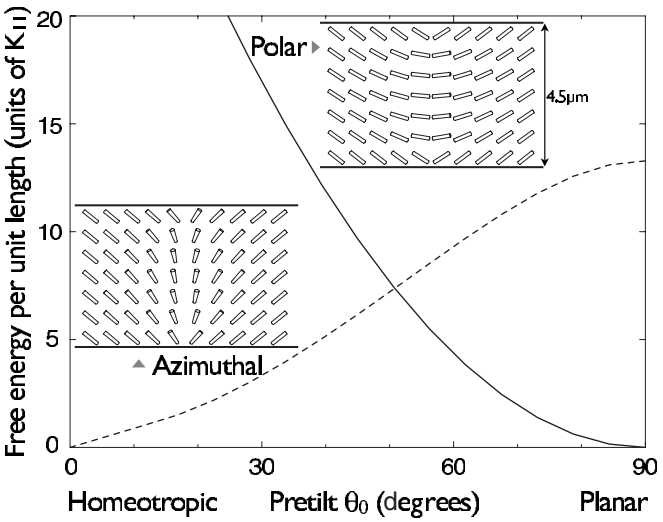

FIG. 6. Normalized free energy per unit length of domain wall assuming either a polar variation of the director across the wall (solid line) or azimuthal variation (dashed line). Insets show the director orientation for the two cases. Note that θ_0 is defined as the angle with respect to the *vertical* direction.

Returning to the experiment, we applied an electric field across the cell using indium-tin-oxide coated glass slides as the substrate for the SE1211 alignment layer, and found that the contrast between the domains and the walls that separate them decreases with increasing voltage. Owing to the negative dielectric anisotropy of the ZLI-4330 liquid crystal, an increase in applied voltage tends to increase the polar angle θ of the director in the bulk. Although varying θ with an applied electric field is not identical to varying θ with temperature through the temperature dependence of the pretilt angle θ_0—this is because θ varies with z in the presence of an applied voltage—the qualitative effect is similar: The contrast decreases at larger values of θ, resulting from an increase in either temperature or voltage.

An interesting observation involves the color spectrum of the domains. In order to exclude the possibility of twist about an axis normal to the cell, we constructed a cell in which the SE1211 was underbaked, resulting in a homeotropic director orientation of ZLI-4330 at room temperature [8]. On applying a voltage, the director underwent a polar tilt, and the resulting color of the domains observed under crossed polarizers was decomposed into red, blue, and green. At a given voltage it was possible to match the RGB values for the voltage-driven cell with the RGB values for the reverse tilt domain cell at room temperature. Then, on heating the RTD cell (and thereby increasing θ_0), it was possible to match the RGB values for the voltage-driven cell at a higher voltage. This exercise was performed over a wide temperature range approaching the isotropic phase, the results showing conclusively that the color of the domains is due to a retardation effect, and an absence of rotation.

In conclusion, naturally occurring reverse tilt domains have been observed and analyzed. Their appearance is due to the large pretilt angle θ_0, i.e., nearly planar director orientation of the director, when the liquid crystal is cooled imme-

diately below the clearing temperature T_{NI}. This results in a lowest energy configuration in which $|\theta|$ undergoes a polar variation across the domain wall through the angle $\theta=90°$ (the planar direction). On further cooling, the pretilt angle decreases (the director transits from nearly planar to nearly vertical orientation), but the reverse tilt domains and their filamentlike walls remain due to the topological barrier that prevents the formation of an azimuthal variation of the director between tilt domains. In previous work we demonstrated that the nonzero pretilt θ_0 derives from the competition between two easy axes [9,10], one nearly vertical and one nearly planar, and that the azimuthal orientation is guided weakly by the local orientation of the polymer backbone. In the absence of rubbing—or other means to enforce a spatially homogeneous planar alignment throughout the cell—there is no well-defined mechanism to choose a tilt angle $+\theta_0$ or $-\theta_0$, and therefore the filamentlike domain walls appear without additional cell preparation. The textures are found to be temporally robust, lasting at least 14 days, as they are topologically stable and are pinned by surface memory effects—even after the cell is heated into the isotropic and recooled into the nematic phase.

The authors thank Ichiro Kobayashi of Nissan Chemical Industries, Ltd. for useful discussions and for providing the alignment material SE1211. This work was supported by the National Science Foundation under Grant No. DMR-0345109.

[1] J. Chen, P. J. Bos, D. R. Bryant, D. L. Johnson, S. H. Jamal, and J. R. Kelly, Appl. Phys. Lett. **67**, 1990 (1995).
[2] C. Fraser, J. Phys. A **11**, 1439 (1978).
[3] D. K. Shenoy, J. V. Selinger, K. A. Grüneberg, J. Naciri, and R. Shashidhar, Phys. Rev. Lett. **82**, 1716 (1999).
[4] Seo Hern Lee, Tae-Hoon Yoon, Jae Chang Kim, and Gi-Dong Lee, J. Appl. Phys. **100**, 064902 (2006).
[5] N. A. Clark, Phys. Rev. Lett. **55**, 292 (1985).
[6] Y. Ouchi, M. B. Feller, T. Moses, and Y. R. Shen, Phys. Rev. Lett. **68**, 3040 (1992).
[7] R. Yamaguchi and S. Sato, Jpn. J. Appl. Phys., Part 2 **39**, L681 (2000).
[8] G. P. Sinha, B. Wen, and C. Rosenblatt, Appl. Phys. Lett. **79**, 2543 (2001).
[9] T. Shioda, B. Wen, and C. Rosenblatt, Phys. Rev. E **67**, 041706 (2003).
[10] G. Carbone and C. Rosenblatt, Phys. Rev. Lett. **94**, 057802 (2005).
[11] A. Rapini and M. Papoular, J. Phys. (Paris), Colloq. **30**, C4-54 (1969).
[12] P. G. DeGennes and J. Prost, *The Physics of Liquid Crystals* (Clarendon, Oxford, 1993).
[13] Manufacturer (Merck's) data sheet for material ZLI-4330.
[14] L. M. Blinov, A. Yu. Kabayenkov, and A. A. Sonin, Liq. Cryst. **5**, 645 (1989).
[15] Bing Wen and C. Rosenblatt, J. Appl. Phys. **89**, 4747 (2001).